HAL
archives-ouvertes.fr

Observation of the stepwise blue shift of a dispersive wave preceding its trapping by a soliton

A. Bendahmane, A. Mussot, M. Conforti, A. Kudlinski

▶ To cite this version:

HAL Id: hal-02389190
https://hal.archives-ouvertes.fr/hal-02389190

Submitted on 2 Dec 2019

Observation of the stepwise blue shift of a dispersive wave preceding its trapping by a soliton

A. Bendahmane, A. Mussot, M. Conforti and A. Kudlinski[*]

Laboratoire PhLAM, UMR CNRS 8523, IRCICA, USR CNRS 3380, Université Lille 1
59655 Villeneuve d'Ascq, France
[*]*alexandre.kudlinski@univ-lille1.fr*

Abstract: The trapping of a weak dispersive wave by an intense soliton is a complex process occurring at the early stage of supercontinuum generation. It is theoretically predicted to arise from multiple soliton-dispersive wave interactions, producing a stepwise frequency blue shift of the dispersive wave. We report here the first experimental evidence of this frequency blue shift using a tapered fiber which acts as a prism, allowing to disperse the blue spectral components in order to identify unambiguously each soliton-dispersive wave collision.

References and links

1. P. K. A. Wai, C. R. Menyuk, Y. C. Lee, and H. H. Chen, "Nonlinear pulse propagation in the neighborhood of the zero-dispersion wavelength of monomode optical fibers," Opt. Lett. **11**, 464–466 (1986).
2. P. K. A. Wai, C. R. Menyuk, H. H. Chen, and Y. C. Lee, "Soliton at the zero-group-dispersion wavelength of a single-model fiber," Opt. Lett. **12**, 628–630 (1987).
3. N. Akhmediev and M. Karlsson, "Cherenkov radiation emitted by solitons in optical fibers," Phys. Rev. A **51**, 2602–2607 (1995).
4. I. Cristiani, R. Tediosi, L. Tartara, and V. Degiorgio, "Dispersive wave generation by solitons in microstructured optical fibers," Opt. Express **12**, 124–135 (2004).
5. F. M. Mitschke and L. F. Mollenauer, "Discovery of the soliton self-frequency shift," Opt. Lett. **11**, 659–661 (1986).
6. J. C. Travers and J. R. Taylor, "Soliton trapping of dispersive waves in tapered optical fibers," Opt. Lett. **34**, 115–117 (2009).
7. D. V. Skryabin and A. V. Gorbach, "*Colloquium*: Looking at a soliton through the prism of optical supercontinuum," Rev. Mod. Phys. **82**, 1287–1299 (2010).
8. J. M. Dudley, G. Genty, and S. Coen, "Supercontinuum generation in photonic crystal fiber," Rev. Mod. Phys. **78**, 1135–1184 (2006).
9. R. Driben, F. Mitschke, and N. Zhavoronkov, "Cascaded interactions between Raman induced solitons and dispersive waves in photonic crystal fibers at the advanced stage of supercontinuum generation," Opt. Express **18**, 25993–25998 (2010).
10. A. Kudlinski, A. K. George, J. C. Knight, J. C. Travers, A. B. Rulkov, S. V. Popov, and J. R. Taylor, "Zero-dispersion wavelength decreasing photonic crystal fibers for ultraviolet-extended supercontinuum generation," Opt. Express **14**, 5715–5722 (2006).
11. S. T. Sørensen, A. Judge, C. L. Thomsen, and O. Bang, "Optimum fiber tapers for increasing the power in the blue edge of a supercontinuum - group-acceleration matching," Opt. Lett. **36**, 816–818 (2011).
12. A. V. Gorbach and D. V. Skryabin, "Light trapping in gravity-like potentials and expansion of supercontinuum spectra in photonic-crystal fibres," Nat Photon **1**, 653–657 (2007).
13. C. Liu, E. J. Rees, T. Laurila, S. Jian, and C. F. Kaminski, "Periodic interactions between solitons and dispersive waves during the generation of non-coherent supercontinuum radiation," Opt. Express **20**, 6316–6324 (2012).

14. A. V. Yulin, D. V. Skryabin, and P. S. J. Russell, "Four-wave mixing of linear waves and solitons in fibers with higher-order dispersion," Opt. Lett. **29**, 2411–2413 (2004).

15. D. V. Skryabin and A. V. Yulin, "Theory of generation of new frequencies by mixing of solitons and dispersive waves in optical fibers," Phys. Rev. E **72**, 016619 (2005).

16. T. G. Philbin, C. Kuklewicz, S. Robertson, S. Hill, F. König, and U. Leonhardt, "Fiber-optical analog of the event horizon," Science **319**, 1367–1370 (2008).

17. K. E. Webb, M. Erkintalo, Y. Xu, N. G. R. Broderick, J. M. Dudley, G. Genty, and S. G. Murdoch, "Nonlinear optics of fibre event horizons," Nat Commun **5**, 4969 (2014).

18. G. Genty, M. Erkintalo, and J. M. Dudley, "Do optical event horizons really exist? The physics of nonlinear reflection at a soliton boundary," in "Advanced Photonics Congress," (Optical Society of America, 2012), OSA Technical Digest (online), p. NW3D.2.

19. A. V. Gorbach, D. V. Skryabin, J. M. Stone, and J. C. Knight, "Four-wave mixing of solitons with radiation and quasi-nondispersive wave packets at the short-wavelength edge of a supercontinuum," Opt. Express **14**, 9854–9863 (2006).

20. A. V. Gorbach and D. V. Skryabin, "Theory of radiation trapping by the accelerating solitons in optical fibers," Phys. Rev. A **76**, 053803 (2007).

21. G. Genty, M. Lehtonen, and H. Ludvigsen, "Effect of cross-phase modulation on supercontinuum generated in microstructured fibers with sub-30 fs pulses," Opt. Express **12**, 4614–4624 (2004).

22. N. Nishizawa and T. Goto, "Characteristics of pulse trapping by ultrashort soliton pulse in optical fibers across zerodispersion wavelength," Opt. Express **10**, 1151–1160 (2002).

23. N. Nishizawa and T. Goto, "Pulse trapping by ultrashort soliton pulses in optical fibers across zero-dispersion wavelength," Opt. Lett. **27**, 152–154 (2002).

24. A. V. Gorbach and D. V. Skryabin, "Bouncing of a dispersive pulse on an accelerating soliton and stepwise frequency conversion in optical fibers," Opt. Express **15**, 14560–14565 (2007).

25. J. C. Travers, "Blue extension of optical fibre supercontinuum generation," J. Opt. **12**, 113001 (2010).

26. A. Kudlinski and A. Mussot, "Visible cw-pumped supercontinuum," Opt. Lett. **33**, 2407–2409 (2008).

27. K. Saitoh and M. Koshiba, "Empirical relations for simple design of photonic crystal fibers," Optics Express **13**, 267 (2005).

28. F. R. Arteaga-Sierra, C. Milián, I. Torres-Gómez, M. Torres-Cisneros, A. Ferrando, and A. Dávila, "Multi-peak-spectra generation with Cherenkov radiation in a non-uniform single mode fiber," Opt. Express **22**, 2451–2458 (2014).

29. M. Billet, F. Braud, A. Bendahmane, M. Conforti, A. Mussot, and A. Kudlinski, "Emission of multiple dispersive waves from a single Raman-shifting soliton in an axially-varying optical fiber," Opt. Express **22**, 25673–25678 (2014).

30. A. Bendahmane, F. Braud, M. Conforti, B. Barviau, A. Mussot, and A. Kudlinski, "Dynamics of cascaded resonant radiations in a dispersion-varying optical fiber," Optica **1**, 243–249 (2014).

31. M. Conforti, S. Trillo, A. Mussot, and A. Kudlinski, "Parametric excitation of multiple resonant radiations from localized wavepackets," Sci. Rep. **5**, 9433 (2015).

1. Introduction

A soliton propagating near the zero-dispersion wavelength (ZDW) of optical fibers may emit a phase-matched dispersive wave (DW) across it, owing mainly to third-order dispersion (TOD) [1,2]. This occurs when the tail of the soliton spectrum seeds the phase-matching wavelength of the DW, *i.e.* when the overlap between the soliton spectrum and the normal group velocity dispersion (GVD) region is sufficient [3,4]. When the TOD term β_3 is positive, the phase-matching relation ruling this process imposes the soliton to travel ahead of the DW in the time domain. A key ingredient for the soliton-DW interaction to occur is thus the deceleration of the soliton required to cause their collision. In uniform fibers, this soliton deceleration naturally occurs through Raman-induced soliton self-frequency shift (SSFS) towards lower group velocity spectral regions [5]. In tapered fibers, the axially-varying group velocity may further enhance the deceleration of the soliton, additionally to the Raman effect [6]. The subsequent nonlinear mixing [7] occurring during the collisions between the soliton and the DW is at the heart of the supercontinuum (SC) generation process in optical fibers [7–9]. This is the main physical process at the origin of the ultraviolet SC extension [6, 10, 11].

Consequently, soliton-DW interactions have been extensively studied to get a deeper understanding of the underlying physics of SC generation [7, 8] (and references therein these review

papers). Once the DW catches up with the tail of the decelerating soliton in the time domain, the latter acts as a potential barrier which scatters the DW and causes its reflection [12, 13]. As a consequence, the DW decelerates and its group velocity decreases. Since DWs are generated in the normal dispersion region, then decreasing group velocity occurs for decreasing wavelengths, so that the reflected DW has to be blue-shifted. This nonlinear mechanism is ruled by a wavenumber matching condition [14, 15] and can be interpreted as an interpulse four-wave mixing (FWM) process, or more surprisingly as an optical analog to event horizons because of the impenetrability of the soliton [16, 17]. However, the potential barrier created by the soliton is finite [7, 12, 13] so that light can leak through it, thus preventing the existence of an ideal optical event horizon in strict sense [18]. This means that at each soliton-DW collision, there is a part of the DW which is transmitted through the soliton in addition to the part which is reflected.

After the first soliton-DW collision, the soliton keeps decelerating, either through SSFS in uniform fibers, or through a combination of SSFS and axially-varying group velocity in tapered fibers [6]. As a consequence, the reflected DW falls back onto the soliton trailing edge and the same collision process repeats many times along propagation [7]. It becomes more and more frequent with fiber length and the blue shift of the reflected DW progressively decreases [13] since the group velocity mismatch between the soliton and the DW reduces [19], until the limit where both group velocities coincide. In other words, the discrete interpulse FWM process describing the cascaded scattering of the DW from the soliton therefore becomes continuous and is termed interpulse FWM process [19]. This corresponds to the trapping of the DW by the soliton [20], sometimes described in terms of cross-phase modulation between the soliton and the DW [8, 21–23]. This transition from interpulse to intrapulse FWM mechanisms has been highlighted in the context of short pulse SC generation [19], and the multiple soliton-DW collisions preceding the full DW trapping have been shown to produce a stepwise frequency blue shift of the DW [13, 24]. However, this process remains yet to be observed experimentally unambiguously, due to the usual presence of a substantial number of solitons and trapped DWs in typical SC experiments.

Our aim here is to investigate the dynamics of a soliton-DW pair and to provide experimental evidence for the multiple collisions occurring before the trapping of the DW by the soliton. To do that, we used a tapered photonic crystal fiber (PCF) that allows to enhance the required soliton deceleration. This leads to an unambiguous identification of each DW in the spectrum.

2. Results

The stepwise frequency blue shift of the DW resulting from its multiple collisions with the soliton at the early stage of SC generation was initially predicted theoretically and numerically [7, 19, 24]. It was then unambiguously identified with numerical simulations using the generalized nonlinear Schrödinger equation (GNLSE) [13]. In this work, the authors used numerical spectrograms in which the DW is well isolated both in time and frequency. This is the only way to easily and carefully capture the DW characteristics, which is difficult to do directly in the spectrum, because reflected radiations from the successive collisions have very close frequencies. As a consequence, these spectral components are often hidden in the SC spectrum [9, 19]. This is further illustrated with the spectrum in grey line in Fig. 1(c), which was simulated for a uniform fiber with the same properties as the input of the tapered fiber described below. The large peak located around 940 nm actually contains four DWs, but they cannot be dissociated in the spectrum because they are too close to each other. This is one of the main reason why they have never been clearly captured experimentally. In the present work, we use a tapered fiber to enhance the Raman-induced soliton deceleration so that collisions occur less frequently along the fiber than they would do in a uniform fiber. The frequency blue shift of

the DW between two collisions is therefore larger. This is reinforced by the fact that the group velocity matching condition with the soliton evolves towards the blue as a results of the axially varying fiber dispersion [6, 25, 26]. As a consequence, the stepwise frequency blue shift of the DW preceding its trapping can be captured unambiguously for the first time experimentally. This is illustrated with the (Visualization 1) file associated to Fig. 1, which shows numerically that the step of the DW frequency blue shift in the output spectrum (right panel) increases when the slope of the tapering section (left panel) increases. This video shows that the taper acts as a prism which disperses the blue part of the output spectrum, thus allowing the spectral signature of the multi-collision process to be captured.

The PCF used in our experiments has an initial 3 m-long uniform section with a pitch Λ of 3.6 μm and relative air hole size d/Λ of 0.75. The pitch then decreases linearly to 3.1 μm over 15 m and is constant over the final 7 m-long section, the d/Λ being constant all along the PCF. Using these parameters of the cross-section structure, we calculated the dispersive and nonlinear properties using the empirical relations from [27]. The black solid line in Fig. 1(d) shows the evolution of the zero dispersion wavelength (ZDW) which decreases from 997 nm at the input to 954 nm at the output, with a linear profile along the tapered section. The nonlinear parameter increases from 17.4 $W^{-1}.km^{-1}$ to 23 $W^{-1}.km^{-1}$ at 1 μm. Experiments were performed using a Ti:Sa oscillator delivering Fourier transform limited gaussian pulses with a full width at half
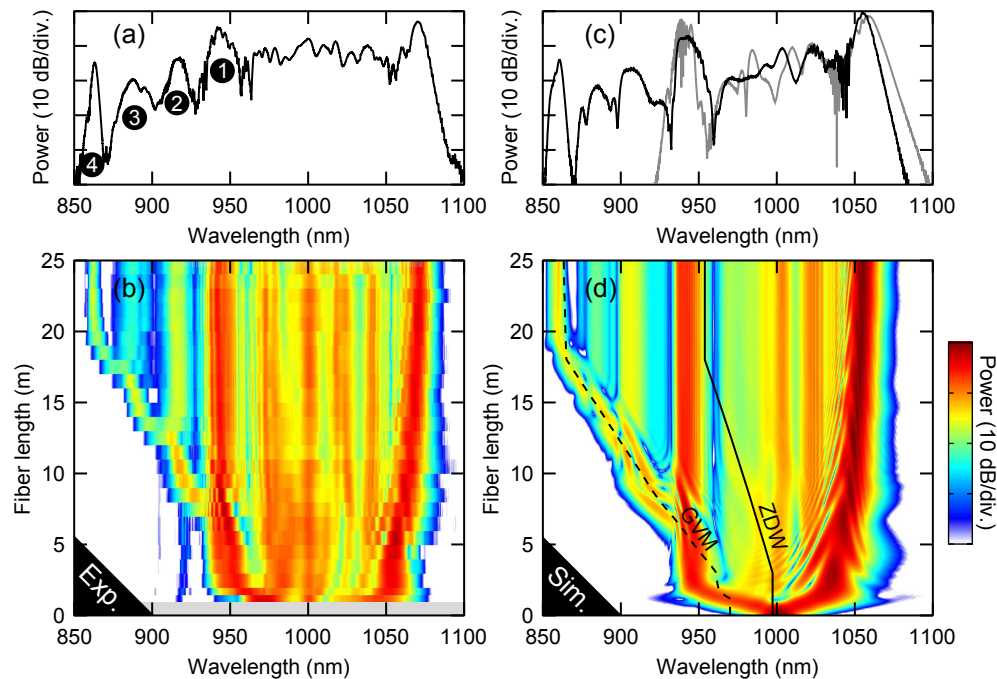

Fig. 1. (a)-(b) Experiments: (a) output spectrum and (b) spectral dynamics along the fiber measured by successive cutbacks. (c)-(d) Corresponding GNLSE simulations: (c) output spectrum and (d) simulated spectral dynamics with fiber length. The grey line in (c) is the simulated output spectrum in a uniform fiber (with the same properties as the input of the tapered fiber described in the text). The colorbar is the same for (b) and (d). In (d), black solid and dashed lines represent respectively the calculated ZDW and the GVM wavelength with the soliton deduced from numerical simulations. (Visualization 1): simulated evolution of the output spectrum (right panel) for increasing slope of the tapering section (left panel).

maximum (FWHM) duration of 116 fs centered at 1001 nm. Figure 1(a) shows the output spectrum measured for a pump average power of 8.7 mW effectively launched into the fiber. The generated SC is relatively flat around the pump wavelength (between 970 and 1050 nm) but it contains isolated peaks on both edges. At the long-wavelength edge, a soliton ejected from the pump pulse is observed at 1070 nm. At the short-wavelength edge, four isolated and distinct peaks are located between 850 and 960 nm.

The spectral dynamics was investigated by recording the output spectrum as a function of fiber length after successive cutbacks of 1 m. The resulting plot is displayed in Fig. 1(a). The red part of the spectrum is identified as a usual Raman shifting soliton. The dynamics of the blue edge is much more complex. First, a DW is emitted by the soliton within the first 3 m (uniform section), following the well-known standard mechanism [1–3]. A part of this DW does not evolve anymore with fiber length, which correspond to the 943 nm peak (labeled #1) in the output spectrum. However, a significant part of the initial DW is suddenly blue-shifted at around 7 m, which corresponds to the 915 nm peak (labeled #2). Similar blue-shifts occur again at 14 m and 17 m, corresponding respectively to the 888 nm and 863 nm peaks (labeled #3 and #4). Figure 2 summarizes these measurements and illustrates the stepwise evolution of the DW peak highlighted in [13]. Black circles correspond to the evolution of the most blue-shifted peak with fiber length. Grey circles represent the longitudinal evolution of other spectral features located at the blue edge of the pump. It can be seen that the peak located at the short-wavelength edge experiences a stepwise blue shift (black circles), and that at each step, a part of the radiation propagates linearly until the fiber output (grey circles).
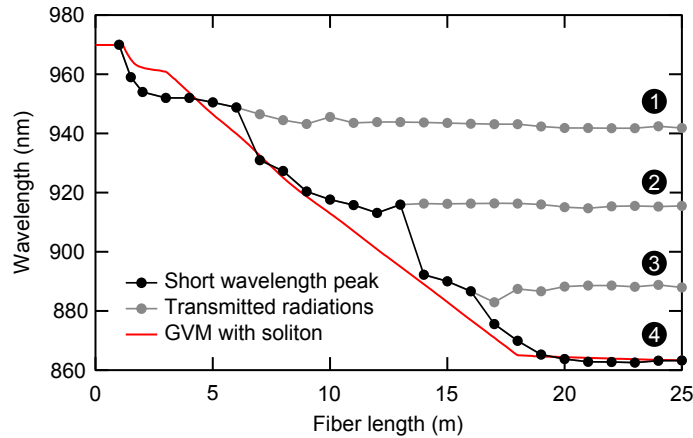

Fig. 2. Measured short wavelength edge (full black circles) and DW wavelength after each collision (full grey circles) as a function of fiber length. The red solid line represents the GVM wavelength with the soliton deduced from numerical simulations.

3. Discussion

In order to investigate the origin of these four blue-shifted peaks, we numerically solved the following GNLSE [8]:

$$i\partial_z A + d(i\partial_t)A + \gamma\left(1 + i\tau_s\partial_t\right)\left(A\int R(t')|A(t-t')|^2\right) = 0, \tag{1}$$

where $d(i\partial_t) = \sum_{n\geq 2}\frac{\beta_n}{n!}(i\partial_t)^n$ is the dispersion operator, γ is the nonlinear parameter, $R(t) = (1-f_R)\delta(t) + f_R h_R(t)$ includes both instantaneous (Kerr) and Raman responses ($f_R = 0.18$),

$\tau_s \approx 1/\omega_p$ is the self-steepening time, ω_p is the pump carrier frequency, around which $d(i\partial_t)$ is expanded, and t is the retarded time in the frame traveling at natural group velocity $V_g = V_g(\omega_p) = \beta_1^{-1}$. The dispersion curve and nonlinear parameter were calculated using the model of [27] as described above. The input field was similar to the one used in experiments (gaussian pulses of 116 fs FWHM duration centered at 1001 nm, with a peak power of 240 W). The output spectrum and the whole spectral dynamics shown respectively in Figs. 1(c) and 1(d), are in good agreement with the measurements. The small discrepancy between the measured and calculated wavelength of the soliton and blue peaks can be attributed to uncertainties in fiber parameters (dispersion and nonlinearity) and/or pump parameters (chirp, power, duration). However, the main spectral features of interest here, and especially the four peaks located at the blue edge, are accurately reproduced in simulations. The first observation is that the blue edge of the spectrum roughly follows the group-velocity matching (GVM) condition with the soliton [represented by the black dashed line in Figs. 1(d)] extracted from the simulation. This is also the case experimentally as can be seen from Fig. 2, where the short wavelength peak (black circles) is shown to oscillate around the GVM condition (represented by the red solid line).

Further information of the process causing these oscillations can be drawn from the simulated temporal evolution of the field shown in Fig. 3. This temporal map was obtained by numerically filtering out all spectral components above 960 nm, in order to highlight the dynamics of the short-wavelength peaks. The temporal trajectory of the soliton is thus represented by the red dashed line. The initial radiation generated near 0 ps correspond to the phase-matched DW emitted by the soliton. The soliton decelerates through the combined effects of Raman scattering and fiber tapering so that it collides with the DW at around 7 m. At this point, a part of the DW is transmitted through the soliton (labeled #1) and another part is reflected on the soliton, causing a frequency conversion of the DW [14, 15]. This collision process between the reflected part of the DW and the soliton occurs again at 14 and 17 m. New spectral components are generated each time. Finally, the remaining part of reflected radiation becomes trapped by the soliton after the end of the tapered section (located at 18 m), because the collisions are more and more frequent and cannot be dissociated from each other anymore [7, 19]. In this
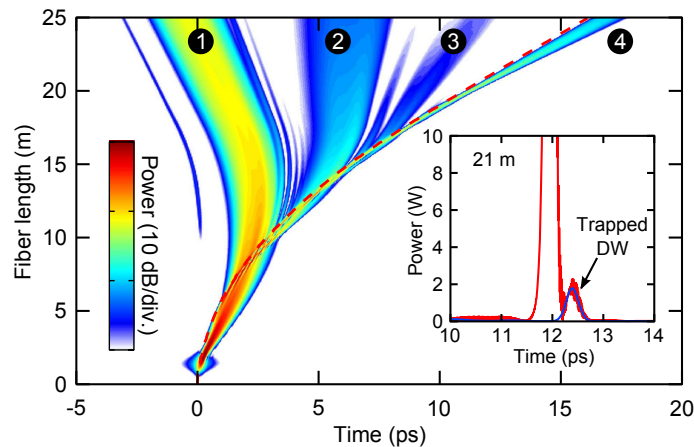

Fig. 3. Simulated temporal evolution of various DWs involved in the multi-collision process. A numerical short-pass filter was used, with a cutoff wavelength of 960 nm in order to highlight the evolution of the DWs. The dashed red line represent the evolution of the soliton central wavelength deduced from numerical simulations of Fig. 1(d). Inset: Simulated full (red line) and filtered (blue line) temporal profile at 21 m

case, the FWM process describing the soliton-DW interaction is not discrete anymore and has been termed *intrapulse* by Gorbach *et al.* [19]. The consequence of this intrapulse FWM process is that the DW remains localized at the trailing edge of the soliton (see inset of Fig. 3) and is trapped in the potential created by the decelerating soliton. This analysis of the time domain map therefore confirms that the multi-peak spectrum observed in our experiments of Figs. 1(a) and 1(b) is due to the multiple soliton-DW collisions preceding the trapping of the DW.

Finally, we would like to point out that multi-peak spectra resulting from soliton-DW interactions have been predicted and observed in various configurations in axially-varying fibers [28–31]. At first view, some of these results may resemble the ones presented in this paper, even though they are actually totally different. Indeed, in Refs. [28, 29], the multi-peak structure of the spectrum below the pump wavelength was due to a soliton hitting the axially-varying ZDW several times along propagation, and therefore generating a new DW each time. Because the soliton wavelength was increasing through SSFS and the dispersion was changing axially, the phase-matching DW wavelength was different each time, creating several DW peaks in the output spectrum. In [30], multiple spectral components were generates through a combination of the previous mechanism and a new one that we termed cascaded DW generation. In [31], multiple DWs were generated by a quasi-phase matching process due to the longitudinal periodic dispersion of the fiber. In all these cases, the n peaks in the spectrum therefore correspond to n distinct DWs, on the contrary to the present study in which they are due to a single DW experiencing successive collisions with the same soliton. Finally, none of these results can be interpreted using the FWM process between the soliton and the DW [14, 15], which is at the heart of the present study.

4. Conclusion

We have experimentally provided the evidence for the multiple soliton-DW collisions leading to a stepwise frequency blue shift of the DW, preceding its trapping by the soliton. This corresponds to the transition from the interpulse to intrapulse FWM mixing between the soliton and the DW, theoretically described by Gorbach *et al.* about ten years ago [19]. This observation was made clear by the use of a tapered fiber enhancing the soliton deceleration so that the spectral components generated at each collision can be unambiguously isolated and measured.